AMP-activated protein kinase-independent inhibition of hepatic mitochondrial oxidative phosphorylation by AICA riboside

Bruno Guigas, Nellie Taleux, Marc Foretz, Dominique Detaille, Fabrizio Andreelli, Benoit Viollet, Louis Hue

Biochemical Journal Immediate Publication. Published on 27 Feb 2007 as manuscript BJ20070105

AMP-activated protein kinase-independent inhibition of hepatic mitochondrial oxidative phosphorylation by AICA riboside

Bruno Guigas*, Nellie Taleux*,†, Marc Foretz‡, Dominique Detaille†, Fabrizio Andreelli‡, Benoit Viollet‡ and Louis Hue*

* Université catholique de Louvain and Institute of Cellular Pathology, Hormone and Metabolic Research Unit, Brussels, Belgium; † Bioénergétique Fondamentale et Appliquée INSERM-EMI0221, Université J. Fourier, Grenoble, France; ‡ Institut Cochin, Université Paris Descartes, CNRS (UMR 8104), Paris, France ; Inserm, U567, Paris, France.

Address for correspondence: *Dr. Bruno Guigas, Department of Molecular Cell Biology, Leiden University Medical Center, Postzone S1-P, Postbus 9600, 2300 RC Leiden, the Netherlands; Tel. +31-71-526 9269; Fax: +31-71-526 8270; E-Mail: b.guigas@lumc.nl*

Running title: AMPK-independent inhibition of OXPHOS by AICA riboside

Abbreviations used: ACC, acetyl-CoA carboxylase; AICA riboside, 5-Aminoimidazole-4-carboxamide-1-β-D-ribofuranoside; AMPK, AMP-activated protein kinase; DNP, 2,4-dinitrophenol; Fru-1-P, fructose 1-phosphate; JO_2, oxygen consumption rate; mtTFA, mitochondrial transcription factor A; OXPHOS, oxidative phosphorylation; PGC-1α, peroxisome activated receptor gamma coactivator 1α; Pi, inorganic phosphate; TMPD, N, N, N', N'-tetramethyl-1, 4-phenylenediamine; ZMP, AICA ribotide

Footnotes: [1]Although strictly speaking, AICAR refers to the nucleotide (AICA ribotide or ZMP, with Z referring to imidazole), it is however often used to designate the corresponding nucleoside (AICA riboside). To avoid any confusion, we use AICA riboside and ZMP in this work.

Biochemical Journal Immediate Publication. Published on 27 Feb 2007 as manuscript BJ20070105

SYNOPSIS

5-Aminoimidazole-4-carboxamide-1-β-D-ribofuranoside (AICA riboside) has been extensively used in cells to activate the AMP-activated protein kinase (AMPK), a metabolic sensor involved in cell energy homeostasis. In this work, we studied its effects on mitochondrial oxidative phosphorylation. AICA riboside was found to dose-dependently inhibit the oligomycin-sensitive oxygen consumption rate (JO_2) of isolated rat hepatocytes. A decrease in inorganic phosphate (Pi), ATP, AMP and total adenine nucleotide contents was also observed with [AICA riboside] > 0.1 mM. Interestingly, in hepatocytes from mice lacking both α1 and α2 AMPK catalytic subunits, basal JO_2 and expression of several mitochondrial proteins were significantly reduced compared to wild-type mice, suggesting that mitochondrial biogenesis was perturbed. However, inhibition of JO_2 by AICA riboside was still present in the mutant mice and thus was clearly not mediated by AMPK. In permeabilized hepatocytes, this inhibition was no longer evidenced, suggesting that it could be due to intracellular accumulation of Z nucleotides and/or loss of adenine nucleotides and Pi. ZMP did indeed inhibit respiration in isolated rat mitochondria through a direct effect on the respiratory-chain complex 1. In addition, inhibition of JO_2 by AICA riboside was also potentiated in cells incubated with fructose to deplete adenine nucleotides and Pi. We conclude that AICA riboside inhibits cellular respiration by an AMPK-independent mechanism that likely results from the combined intracellular Pi depletion and ZMP accumulation. Our data also demonstrate that the cellular effects of AICA riboside are not necessarily caused by AMPK activation and thus that their interpretation should be taken with caution.

Keywords: AMP-activated protein kinase; AICA riboside; Hepatocytes; Mitochondrial oxidative phosphorylation; Mitochondrial biogenesis; ZMP

Biochemical Journal Immediate Publication. Published on 27 Feb 2007 as manuscript BJ20070105

INTRODUCTION

5-Aminoimidazole-4-carboxamide-1-β-D-ribofuranoside (AICA riboside) is the nucleoside corresponding to AICA ribotide (AICAR[1] or ZMP), the antepenultimate metabolic intermediate of the *de novo* purine synthesis pathway. AICA riboside shares some structural similarities with adenosine and enters certain cell types to be phosphorylated into ZMP by adenosine kinase [1, 2]. ZMP is an analogue of AMP and mimics several of the cellular effects of this adenine nucleotide. In recent years, AICA riboside has been extensively used in cells [3, 4] or even *in vivo* [5-9] to activate the AMP-activated protein kinase (AMPK) and assess its function in a large number of pathways.

AMPK is a heterotrimeric protein kinase consisting of a catalytic (α) and two regulatory subunits (β and γ) (see [10, 11] for recent reviews). Considered as a metabolic "fuel gauge", AMPK becomes activated by changes in intracellular adenine nucleotide concentrations, namely a fall in ATP with the resulting increase in AMP concentration, that occur in cells submitted to environmental and nutritional stresses. In the presence of AMP (or ZMP), AMPK can be phosphorylated on Thr172 which is located in the activation loop of its catalytic subunit. This activating phosphorylation can be catalyzed by either LKB1 or the Ca^{2+}/calmodulin-dependent protein kinase kinase β, two protein kinases located upstream of AMPK [10]. Once activated, AMPK inactivates energy-consuming biosynthetic pathways and activates ATP-producing catabolic pathways, thereby maintaining cellular ATP. The importance of the role of AMPK in the control of energy homeostasis is further underlined by its indirect stimulatory effect on mitochondrial biogenesis [12], at least in skeletal muscle [13, 14].

We recently reported that AICA riboside inhibited the glucose-induced translocation of glucokinase from the nucleus to the cytosol in hepatocytes by a mechanism that could be related to a decrease in intracellular ATP concentrations [15]. Therefore, one could wonder whether AICA riboside could affect mitochondrial ATP production, and whether this effect is mediated by AMPK. The aim of this work was to test this hypothesis by studying the effects of AICA riboside on the mitochondrial oxidative phosphorylation (OXPHOS) pathway in hepatocytes from both rat, and wild-type or newly engineered liver specific AMPK$\alpha_1\alpha_{2LS}^{-/-}$ mice.

MATERIALS & METHODS

Generation of AMPK$\alpha_1\alpha_{2LS}^{-/-}$ knockout mice. To obtain a deletion of both catalytic subunits in the liver (AMPK$\alpha_1\alpha_{2LS}^{-/-}$), we first generated a liver-specific AMPKα_2-null mouse (AMPK$\alpha_2^{-/-}$) by crossing floxed AMPKα_2 mice [16] and AlfpCre transgenic line expressing the Cre recombinase under control of the albumin and α-fetoprotein regulatory elements [17]. We then produced a liver-specific AMPK$\alpha_1\alpha_{2LS}^{-/-}$ mouse on an AMPK$\alpha_1^{-/-}$ background by crossing liver-specific AMPK$\alpha_2^{-/-}$ mice with AMPK$\alpha_1^{-/-}$ mice [18]. Mice were genotyped by PCR on DNA extracted from a tail biopsy using specific primers for the Cre transgene and for the floxed AMPKα_2, the deleted AMPKα_1 and the wild-type AMPKα_1 gene.

Isolation of hepatocytes. Liver cells were prepared by the collagenase method [19] from male Wistar rats (200-300 g) or from male mice (25-30 g) after anaesthesia with sodium pentobarbital (6 mg/100 g body weight) or ketamin/xylazin (8/1 mg/100 g body weight) respectively.

Isolation of rat mitochondria. Liver mitochondria from male Wistar rats (200-300 g) were prepared in sucrose medium (250 mM sucrose, 1 mM EGTA, 20 mM Tris-HCl, pH 7.2) according to the standard method described by Klingenberg and Slenczka [20]. Mitochondrial proteins were estimated by the Biuret method using bovine serum albumin as a standard.

Determination of mitochondrial oxygen consumption rate in intact and permeabilized hepatocytes and isolated mitochondria. Rat or mouse hepatocytes (7-8 mg dry cells.ml^{-1}) were incubated in a shaking water bath at 37°C in closed vials containing 2 ml Krebs-Ringer-bicarbonate-calcium buffer (120 mM NaCl, 4.8 mM KCl, 1.2 mM KH_2PO_4, 1.2 mM $MgSO_4$, 24 mM $NaHCO_3$, 1.3 mM $CaCl_2$, pH 7.4) supplemented with the indicated concentrations of substrates and AICA riboside, and in equilibrium with a gas phase containing O_2/CO_2 (19:1). At the indicated times, the cell suspension was saturated again with O_2/CO_2 for one min and immediately transferred into a stirred oxygraph vessel equipped with a Clark oxygen electrode. The oxygen consumption rate (JO_2) was measured at 37°C before and after successive addition of 0.5 µM oligomycin, 150 µM 2,4-dinitrophenol (DNP), 0.15 µg/ml antimycin and 1 mM N, N, N', N'-tetramethyl-1,4-phenylenediamine (TMPD) plus 5 mM ascorbate.

To permeabilize hepatocytes, intact cells from mice (7-8 mg dry cells.ml^{-1}) were first incubated for 30 min as described above, then harvested by centrifugation and resuspended in KCl medium (125 mM KCl, 20 mM Tris-HCl, 1 mM EGTA and 5 mM Pi-Tris, pH 7.2) containing 200 µg/ml digitonin. After 3 min at 37°C, the permeabilized hepatocytes were transferred in the oxygraph vessel. As indicated, 5 mM glutamate-Tris plus 2.5 mM malate-Tris or 5 mM succinate-Tris plus 0.5 mM malate-Tris plus 1.25 µM rotenone were added. JO_2 was measured before and after the successive additions of 1 mM ADP-Tris, 0.5 µg/ml oligomycin, 50 µM DNP, 0.15 µg/ml antimycin and 1 mM TMPD plus 5 mM ascorbate, to determine the phosphorylating (state 3), the non-phosphorylating (state 4) and the uncoupled respiratory rate, and the maximal activity of cytochrome oxidase, respectively. In all experiments, the antimycin-sensitive JO_2, which corresponds to mitochondrial respiration, was calculated by subtracting the antimycin-insensitive JO_2 from the total JO_2.

For mitochondrial experiments, isolated rat mitochondria (1 mg protein.ml^{-1}) were incubated at 37 °C in the oxygraph vessel containing 2 ml of the KCl medium described above in the presence of 1 mM AICA riboside or the indicated concentrations of ZMP and ZTP. After equilibration (30 s), mitochondrial respiratory rate was monitored in the presence of glutamate/malate or succinate/malate/rotenone, as described above for permeabilized hepatocytes.

Determination of complex 1 and citrate synthase activities. The specific activity of the respiratory-chain complex 1 was assessed in disrupted mitochondria following hypoosmotic shock by the rotenone-sensitive oxidation rate of NADH in the presence of decylubiquinone as electron acceptor [21]. Citrate synthase activity was measured on liver homogenate, as described [22]. The activities are expressed as nmol.min^{-1}.mg protein^{-1} (complex 1) or µmol.min^{-1}.g protein^{-1} (citrate synthase), the protein contents being determined by the Pierce BCA kit (Rockford, Illinois, USA).

Determination of nucleotides and inorganic phosphate concentrations, and of gluconeogenesis and ketogenesis. After 30 min of incubation, samples of the cell suspension were quenched in ice-cold $HClO_4$-EDTA (5 % w/v - 25 mM) and centrifuged (13000 x g for 2 min). The supernatants were neutralized and adenine nucleotides, ZMP and AICA riboside concentrations

were measured by high performance liquid chromatography [23]. To measure intracellular Pi, 0.7 ml sample of the cell suspension were centrifuged through a silicon oil layer into 0.25 ml of $HClO_4$ – EDTA (10 % w/v / 25 mM). Pi was measured colorimetrically [24]. For gluconeogenesis and ketogenesis measurements, samples of the cell suspension were quenched in ice-cold $HClO_4$ (5 % w/v), centrifuged (13000 x g for 2 min) and the supernatants were neutralized. Glucose, acetoacetate and β-hydroxybutyrate concentrations were measured by enzymatic methods coupled with spectrophotometric determinations of NADH, as described [23].

AMPK assay. Total AMPK activity from hepatocyte extracts was assayed after precipitation with 10% (w/v) polyethylene glycol 6000 [15].

Western blot analysis. Expression of cytochrome c and cytochrome oxidase subunit IV (COX IV) and phosphorylation state of acetyl-CoA carboxylase (ACC) were monitored by SDS-PAGE immunoblots with anti-cytochrome c (clone 7H8.2C12, BD Biosciences), anti-cytochrome oxidase, subunit IV (Cell Signaling) and anti-phosphoSer79 ACC (Upstate) antibodies, respectively. Expression of α-actin (Santa Cruz) was used as loading control. Quantification was performed by densitometry using Image J 1.32 (NIH, USA).

RNA purification and quantitative Reverse Transcription-coupled real-time PCR. Total RNA was isolated with RNA+ (Qbio-gene), and single-strand cDNA was synthesized from 5 μg of total RNA with random hexamer primers and Superscript II (Invitrogen). Real-time RT-PCRs were carried out with a LightCycler reaction kit (Eurogentec) in a final volume of 20 μl containing 250 ng of reverse-transcribed total RNA, 500 $nmol.l^{-1}$ of primers, 10 μl of 2x PCR mix, and 0.5 μl of Sybr Green. The reactions were carried out in a LightCycler instrument (Roche) with 40 cycles. The relative amounts of the mRNAs studied were determined by means of the second-derivative maximum method, using LightCycler analysis software version 3.5 and β-actin as invariant control. The primer sequences used were listed in supplementary Table 1.

Statistics. The results are expressed as means ± SEM for the indicated number of separate experiments. The statistical significance of differences was calculated using Student's test or ANOVA followed by Fisher's protected least significant post hoc test (Statview 5.0.1., SAS

Institute Inc., USA).

RESULTS

Inhibition of oxygen consumption rate by AICA riboside in rat hepatocytes. In a first set of experiments we studied the time-course of AICA riboside effects on intracellular ZMP accumulation, AMPK activation and cellular oxygen consumption rate (JO_2). As expected [2, 4], incubation of hepatocytes with 1 mM AICA riboside resulted in a progressive increase in intracellular ZMP level (up to 20-25 µmol.g dry cells^{-1} after 30 min) with a parallel decrease in the concentration of AICA riboside in the medium, presumably due to its phosphorylation by adenosine kinase (Fig. 1A-B). The activation of AMPK was very rapid and maximal within 2.5 min of incubation (Fig. 1C), suggesting that modest (<3 µmol.g dry cells^{-1}) intracellular accumulation of ZMP would be sufficient to activate AMPK. This was confirmed by the concomitant increase in the phosphorylation state of ACC, one of the main downstream targets of AMPK (Fig. 1C, insert). Interestingly, in parallel with ZMP accumulation, AICA riboside decreased JO_2 of intact hepatocytes, this effect being slower than AMPK activation and maximal after about 20 min (Fig. 1D).

Incubation of hepatocytes with increasing concentrations of AICA riboside was then performed in order to investigate the mechanism of inhibition of JO_2 by the nucleoside. After 30 min of incubation, AICA riboside induced a dose-dependent inhibition of the basal JO_2 (Table 1a), which was already detectable at 0.05 mM AICA riboside. This effect was abolished after addition of oligomycin, an inhibitor of the F0 subunit of ATP synthase, suggesting that the inhibition of JO_2 by AICA riboside was likely due to an alteration of a mitochondrial process linked to ATP synthesis. In agreement with this interpretation, we observed that the calculated oligomycin-sensitive JO_2 (basal minus oligomycin-insensitive JO_2), which represents the cellular oxygen consumption linked to ATP synthesis, was indeed significantly decreased whatever the concentration of AICA riboside used (Table 1a). Furthermore, addition of DNP, which uncouples the mitochondrial OXPHOS, increased JO_2, even in the presence of AICA riboside. This clearly indicates that the inhibitory effect of AICA riboside on JO_2 was not present when the thermodynamic constraint on ATP synthesis was abolished by uncoupling, except at high concentration of the nucleoside. Finally, the lack of effect of AICA riboside in the presence of TMPD/ascorbate, which assesses the maximal activity of cytochrome oxidase, indicated that the nucleoside did not affect this complex of the mitochondrial respiratory-chain (Table 1a). Taken together, our results suggest that the inhibition of cellular JO_2 by AICA riboside was exerted on

step(s) linked to ATP synthesis rather than on the electron transfer chain.

Because AICA riboside could interfere with ATP synthesis, the concentrations of adenine nucleotides were measured. The dose-dependent inhibition of JO_2 by AICA riboside was accompanied by a decrease in ATP and AMP, a slight increase in ADP and a decrease in the total concentration of adenine nucleotides (Table 1b). The ATP-to-ADP ratio was significantly decreased by AICA riboside at concentrations larger than 0.1 mM. Furthermore, at these concentrations of AICA riboside, there was also a large decrease in intracellular Pi. Under these conditions, the gluconeogenic and ketogenic fluxes were drastically reduced, thus reflecting the perturbations in cellular energy metabolism induced by AICA riboside (data not shown).

Interestingly, the inhibition of oligomycin-sensitive JO_2 by AICA riboside was observed whatever the substrates used and was also reversed by DNP addition, except in presence of glucose alone (Table 2).

The inhibition of oxygen consumption rate by AICA riboside is independent of AMPK. To evaluate AMPK involvement in the inhibitory effect of AICA riboside on JO_2, we resorted to engineered mice that were totally deficient in the α_1 isoform of the AMPK catalytic subunit and whose expression of the α_2 isoform was specifically deleted in the liver by Cre-recombinase technology ($AMPK\alpha_1\alpha_{2LS}^{-/-}$). We first confirmed that incubation of hepatocytes isolated from wild-type mice with 1 mM AICA riboside led to AMPK activation (Fig. 2A) and decreased both oligomycin-sensitive JO_2 (Fig. 2C) and ATP (Fig. 2B). The extent of these effects was similar to those observed in rat hepatocytes and the inhibition of JO_2 by AICA riboside was also reverted by addition of DNP (Fig. 2C). In hepatocytes from $AMPK\alpha_1\alpha_{2LS}^{-/-}$ mice, AMPK expression, activity and activation could not be detected (Fig. 2A) but the inhibition of the oligomycin-sensitive JO_2 by AICA riboside persisted (Fig. 2D), excluding an effect mediated by AMPK.

Interestingly, the significant decrease in basal JO_2 evidenced in $AMPK\alpha_1\alpha_{2LS}^{-/-}$ mice compared to wild-type (Fig. 2C and 2D) seemed to be due to a lower total oxidative capacity linked to a decreased cellular mitochondrial content. Indeed, we found a significant decrease in protein expression of both cytochrome c and the subunit IV of the cytochrome oxidase in $AMPK\alpha_1\alpha_{2LS}^{-/-}$ compared with wild-type mice (Fig. 2E-F). To note, the basal level of ATP in $AMPK\alpha_1\alpha_{2LS}^{-/-}$ mice was also significantly lower than in wild-type mice and the decrease induced by AICA riboside was even more pronounced. These results are in line with those

previously reported for primary cultures of hepatocytes from wild-type and AMPK$\alpha_1\alpha_{2LS}^{-/-}$ mice treated with AICA riboside [15]. The decrease in hepatic mitochondrial content evidenced in AMPK$\alpha_1\alpha_{2LS}^{-/-}$ mice, which is also confirmed by a significant decrease in citrate synthase activity (114±6 *vs* 85±5 μmol.min^{-1}.g protein^{-1} in wild-type and AMPK$\alpha_1\alpha_{2LS}^{-/-}$ mice, respectively; $p<0.05$), could be due to an alteration of mitochondrial biogenesis since liver expression of most of the genes involved in this pathway were reduced (Fig. 2G), including the key transcriptional cofactor peroxisome activated receptor gamma coactivator 1α (PGC-1α).

Lack of inhibition of mitochondrial oxidative phosphorylation by AICA riboside in permeabilized hepatocytes. The effect of AICA riboside in intact cells from wild-type and AMPK$\alpha_1\alpha_{2LS}^{-/-}$ mice was further investigated after permeabilization of the plasma membrane by digitonin, allowing the mitochondrial OXPHOS pathway to be investigated *in situ*. Mean values of mitochondrial antimycin-sensitive respiratory rates are given in Table 3. In the presence of glutamate/malate, a substrate for the respiratory-chain complex 1, no significant difference in mitochondrial respiratory rates could be detected after AICA riboside pre-treatment in both wild-type and AMPK$\alpha_1\alpha_{2LS}^{-/-}$ mice and whatever the mitochondrial energy state. Similar results were obtained with succinate/malate, a substrate for the respiratory-chain complex 2. Taken together, these results demonstrate that the inhibition of JO_2 by AICA riboside required cell integrity and was lost in permeabilized cells. The results were similar in AMPK$\alpha_1\alpha_{2LS}^{-/-}$ and also confirmed an overall decrease in mitochondrial respiration in hepatocytes compared to wild-type mice.

Mechanism of inhibition of oxidative phosphorylation by AICA riboside in intact cells. The lack of inhibition of respiration by AICA riboside in permeabilized hepatocytes suggested that the inhibition in intact cells could result from the intracellular accumulation of small molecular mass compounds, such as Z nucleotides, that could have been lost by permeabilization. We first investigated the effects of Z nucleotides on mitochondrial OXPHOS pathway (Table 4). In rat mitochondria energized with glutamate/malate, but not with succinate/malate, ZMP significantly inhibited state 3 respiration. This inhibition persisted in the presence of DNP, which was not the case in intact cells. In addition, incubation of disrupted mitochondria with ZMP significantly decreased the specific activity of the respiratory-chain complex 1 (78±4, 69±4 and 62±3 nmol.min^{-1}.mg protein^{-1} for control, 1 mM and 2.5 mM ZMP, respectively; $p<0.05$),

demonstrating a direct inhibition of this mitochondrial complex by the nucleotide. By contrast, ZTP stimulated mitochondrial respiration whatever the substrate and the mitochondrial energy states (Table 4).

Alternatively, the inhibition of oligomycin-sensitive JO_2 could result from the AICA riboside-induced depletion of substrates for the mitochondrial OXPHOS, such as adenine nucleotides and Pi. This situation is reminiscent of the depletion of adenine nucleotides induced by fructose in hepatocytes [25]. To test this hypothesis, we evaluated the effect of AICA riboside on JO_2 in hepatocytes pre-incubated with 5 mM fructose to decrease intracellular Pi (Table 5). Fructose pre-treatment indeed worsened the relative inhibition of oligomycin-sensitive JO_2 by AICA riboside (-51 % *vs* -63 %, $p<0.05$; control *vs* fructose). In these cells, pre-incubation with fructose also worsened the AICA riboside-induced depletion of ATP and total adenine nucleotides and decreased ATP-to-ADP ratio, thus making it difficult to unequivocally assign to Pi depletion the inhibition of cellular respiration.

To assess the importance of adenine nucleotide depletion in the AICA riboside-induced inhibition of JO_2, we resorted to deoxycoformycin, a known inhibitor of AMP deaminase. This enzyme is inhibited by Pi and limits the breakdown of adenine nucleotides in the liver. Therefore, any depletion of intracellular Pi relieves the inhibition on AMP deaminase and favors adenine nucleotide breakdown, as it occurs in fructose or AICA riboside treated hepatocytes (Table 5). Pre-incubation of hepatocytes with 10 µM deoxycoformycin prevented ATP and total adenine nucleotides depletion, but did not affect the AICA riboside-induced Pi drop (-65 % *vs* -62 %), the decrease in ATP-to-ADP ratio and the inhibition of oligomycin-sensitive JO_2 (Table 5).

Taken together these results suggest that the depletion of Pi that follows phosphorylation of AICA riboside into ZMP also participates in the inhibition of cellular respiration by the nucleoside. Finally, the clear relationship evidenced between intracellular Pi and oligomycin-sensitive JO_2 (Fig. 3) further reinforces this proposed mechanism.

DISCUSSION

We report here that AICA riboside, which is classically used to activate AMPK in cells, was unexpectedly found to inhibit respiration in intact hepatocytes. This effect was readily observed at concentrations of AICA riboside higher than 0.1 mM and was clearly not mediated by AMPK since it persisted in hepatocytes isolated from AMPK$\alpha_1\alpha_{2LS}^{-/-}$ mice. We propose that this inhibition resulted from the combined decrease in intracellular Pi concentration and the accumulation of Z nucleotides following AICA riboside phosphorylation.

Incubation of hepatocytes with AICA riboside induced major changes in nucleotides and Pi content similar to those caused by the accumulation of fructose 1-phosphate (Fru-1-P) and glycerol 3-phosphate (Gly-3-P) in hepatocytes incubated with fructose [25] and glycerol [26], respectively. ZMP resulting from the phosphorylation of AICA riboside by adenosine kinase acts as a Pi trap, like Fru-1-P and Gly-3-P, thus leading to depletion of free Pi and adenine nucleotides. Indeed, rough estimation of the intracellular phosphate charge indicates that the amount of free and adenine nucleotides-bound Pi decreased from about 45 in controls to about 30 μmol.g dry cells^{-1} after incubation with 1 mM AICA riboside, the difference being recovered in the Z nucleotides, mainly ZMP (Table 1). This is in agreement with previous report showing that the liver concentration of free Pi decreased by 50% after *in vivo* administration of AICA riboside and was accompanied by a concomitant and dose-dependent drop in ATP levels owing to the marked accumulation of phosphorylated compounds [27]. The immediate consequences of this Pi depletion is the de-inhibition of AMP deaminase resulting in the loss of adenine nucleotides (Table 1b) and the expected breakdown of the purine ring into allantoïn, as reported [28, 29]. Interestingly, use of deoxycoformycin, an inhibitor of AMP deaminase, abolishes the AICA riboside-induced decrease in adenine nucleotides but not of Pi and JO_2 (Table 5).

Collectively, our results suggest that the main changes induced by AICA riboside, namely the accumulation of ZMP and the depletion of intracellular Pi, are responsible for the inhibition of cellular respiration. In intact cells incubated with lactate/pyruvate and octanoate as substrates, the decrease in JO_2 induced by AICA riboside was relieved under uncoupled conditions, *i.e.* addition of DNP, indicating that the inhibition was mainly exerted on respiration coupled to ATP synthesis in this condition. Since JO_2 is expected to slow down when the concentration of mitochondrial OXPHOS co-factors are limiting [30], the massive drop of Pi following AICA riboside phosphorylation constitutes an attractive explanation. The tight relationship evidenced

between its intracellular content and the oligomycin-sensitive JO_2 illustrates this functional hypothesis.

Accumulation of Z nucleotides, which occurred in all AICA riboside-treated cells, could also participate in the inhibition through a direct effect on the mitochondrial respiratory chain. ZMP was indeed found to inhibit the complex 1 of the respiratory chain in isolated liver mitochondria (Table 3). Such an effect would decrease JO_2 in intact hepatocytes, even after addition of the uncoupler DNP, since inhibition of complex 1 induce kinetic constraint on the entire electron transport chain. However, inhibition of JO_2 by AICA riboside in presence of DNP was only observed with glucose alone, a substrate providing almost exclusively NADH to the mitochondrial respiratory-chain complex 1. In hepatocytes incubated with substrates providing both NADH and $FADH_2$ with a closely related stochiometry, *i.e* glycerol or fatty acid, this effect was probably masked, except at very high concentration, because of the partial bypass of complex 1 [31]. In addition, ZTP, which accumulates in hepatocytes theoretically 10 time less than ZMP [2], induced stimulation of mitochondrial state 4 respiratory rate. This suggests an uncoupling of mitochondrial OXPHOS (Table 3), an effect that could also worsen the change in cellular energetics by decreasing the yield of ATP synthesis. Importantly, all these effects were observed at concentrations of ZMP and ZTP in the range of those detected in isolated hepatocytes incubated by AICA riboside. Indeed, assuming an intracellular water content of 2 $ml.g^{-1}$ dry weight, ZMP and ZTP can reach intracellular concentrations higher than 7.5 and 0.75 mM, respectively, in cells exposed 30 min to 1 mM AICA riboside. Finally, although OXPHOS inhibition by AICA riboside can readily be explained by the observed changes in Pi and ZMP concentrations, other effects of Z nucleotides, *e.g.* on ATP synthase, adenine nucleotide translocator or Pi transporter, are not excluded..

To note, the inhibition of oligomycin-sensitive respiration by AICA riboside was not restricted to hepatocytes and was also observed in various cell lines, including C2C12, CaCo-2, KB and also human endothelial cells (HMEC-1) (data not shown). The common phenomenon shared by these cells is their capacity to accumulate ZMP but the extent of JO_2 inhibition induced by AICA riboside was rather low compared with fresh hepatocytes. However, these culture cell lines generally exhibit high glycolytic rates and are therefore less dependent on mitochondrial OXPHOS for ATP supply. The energetic consequences of the AMPK-independent inhibition of OXPHOS by AICA riboside in these cells are therefore expected to be less important than in liver

cells. Thus, the alteration of OXPHOS pathway by AICA riboside and the subsequent intracellular ATP drop could explained, at least in part, the detrimental effect of the nucleoside treatment evidenced in highly aerobic tissues, *i.e.* in liver [32] or pancreatic cells [33, 34]. By contrast, we can suggest that the protection against apoptosis exerted by AICA riboside in some culture cell lines [35-37] could be due to subtle mitochondrial modifications induced by Z nucleotides. Indeed, moderate inhibition of electron flux through the respiratory-chain complex 1, as evidenced with ZMP, has been demonstrated to protect cells against oxidative stress-induced cell death [21, 38].

It is obvious from our results that caution should be exerted when interpreting the results obtained with AICA riboside and assumed to result from AMPK activation. Among the AMPK-independent but AICA riboside-induced effect, intracellular accumulation of ZMP has been also reported to directly modulate enzymes with AMP binding sites, such as glucokinase [39], glycogen phosphorylase [40, 41], glycogen synthase [40] or fructose 1,6-bisphosphatase [2]. The K_m of these enzymes for ZMP were indeed generally in the range of the cellular nucleotide concentration, a point which was often overlooked in the interpretation of the results obtained with AICA riboside. Two recent papers also reported AMPK-independent effects of AICA riboside on hepatic phosphatidylcholine synthesis [42] and autophagic proteolysis [43], without however providing any mechanistic explanation for these non specific effects.

The striking lower basal JO_2 in hepatocytes from AMPK$\alpha_1\alpha_{2LS}^{-/-}$ compared to wild-type mice is likely due to a decrease in mitochondrial content rather than a qualitative modification of the mitochondrial machinery. Indeed, no differences were evidenced in both cellular (Figure 2) and mitochondrial (Table 3) respiration when the results were normalized using the maximal activity of cytochrome oxidase (data not shown), a usual marker of cellular mitochondrial density. AMPK has been reported to be involved in muscle mitochondrial biogenesis [13, 14] and our results suggest for the first time that this also the case for the liver. Indeed, the deletion of both AMPKα subunits in hepatocytes leads to reduced mitochondrial respiration and decreased transcript and protein expression of key mitochondrial constituents, delineating an apparent alteration of the starvation-induced activation of the mitochondrial biogenesis program in the liver of this mice. PGC-1α [44] and myc [45] have been recently identified as key transcriptional cofactors involved in this pathway since they coordinate activation of several transcription factors, including nuclear respiratory factors and mitochondrial transcription factor A (mtTFA),

which in turn enhances expression of nuclear and mitochondrial genes encoding mitochondrial proteins [46]. While the mRNA content of myc was not modified, the expression of PGC-1α, together with numbers of nuclear (COX IV, Cytochrome C, UCP2, ATPase) and mitochondrial (COX I) genes, was drastically reduced in AMPK$\alpha_1\alpha_{2LS}^{-/-}$ mice (Figure 2). The mechanisms by which deletion of AMPK in the liver affects PGC-1α expression and mitochondrial biogenesis remain to be elucidated.

In conclusion of this study, while one might consider short-term incubations with low concentrations (< 0.1 mM) of AICA riboside to activate AMPK with little OXPHOS damage, we believe that this compound is not well suited to investigate the consequences of AMPK activation on various cell functions because of its misleading side-effects. Other more specific tools and/or new pharmacological compounds with better AMPK selectivity are required. Among these, genetic approaches including overexpression of negative or constitutively active forms of AMPK [47], use of small interfering RNA [48], and invalidation of the genes coding for the catalytic subunits of the kinase [49] are to be considered, taking into account their inherent limitations. Alternatively, the recent development of new activators of AMPK, apparently devoid of any apparent effect on adenine nucleotide content in primary cultured hepatocytes [50], is of direct interest.

ACKNOWLEDGMENTS

This work was supported by FNRS, the French Community of Belgium, the Belgian Federal Program Interuniversity Poles of Attraction (P5) and the European Union FP6 programm (Exgenesis, LSHM-CT-2004-005272). B. Guigas is recipient of the ICP-"Michel de Visscher" Fellowship and N. Taleux is recipient of a French EURODOC grant of the Région Rhône-Alpes. The authors are grateful to Liliane Maisin and Martine de Cloedt for technical assistance.

REFERENCES

1 Zimmerman, T. P. and Deeprose, R. D. (1978) Metabolism of 5-amino-1-beta-D-ribofuranosylimidazole-4-carboxamide and related five-membered heterocycles to 5'-triphosphates in human blood and L5178Y cells. Biochem. Pharmacol. 27, 709-16

2 Vincent, M. F., Marangos, P. J., Gruber, H. E. and Van den Berghe, G. (1991) Inhibition by AICA riboside of gluconeogenesis in isolated rat hepatocytes. Diabetes 40, 1259-66

3 Sullivan, J. E., Brocklehurst, K. J., Marley, A. E., Carey, F., Carling, D. and Beri, R. K. (1994) Inhibition of lipolysis and lipogenesis in isolated rat adipocytes with AICAR, a cell-permeable activator of AMP-activated protein kinase. FEBS Lett. 353, 33-6

4 Corton, J. M., Gillespie, J. G., Hawley, S. A. and Hardie, D. G. (1995) 5-Aminoimidazole-4-Carboxamide Ribonucleoside - a Specific Method for Activating Amp-Activated Protein-Kinase in Intact-Cells. Eur. J. Biochem. 229, 558-565

5 Christopher, M., Rantzau, C., Chen, Z. P., Snow, R., Kemp, B. and Alford, F. P. (2006) Impact of in vivo fatty acid oxidation blockade on glucose turnover and muscle glucose metabolism during low-dose AICAR infusion. Am. J. Physiol. Endocrinol. Metab. 291, E1131-40

6 Aschenbach, W. G., Hirshman, M. F., Fujii, N., Sakamoto, K., Howlett, K. F. and Goodyear, L. J. (2002) Effect of AICAR treatment on glycogen metabolism in skeletal muscle. Diabetes 51, 567-73

7 Bergeron, R., Previs, S. F., Cline, G. W., Perret, P., Russell, R. R., 3rd, Young, L. H. and Shulman, G. I. (2001) Effect of 5-aminoimidazole-4-carboxamide-1-beta-D-ribofuranoside infusion on in vivo glucose and lipid metabolism in lean and obese Zucker rats. Diabetes 50, 1076-82

8 Iglesias, M. A., Furler, S. M., Cooney, G. J., Kraegen, E. W. and Ye, J. M. (2004) AMP-activated protein kinase activation by AICAR increases both muscle fatty acid and glucose uptake in white muscle of insulin-resistant rats in vivo. Diabetes 53, 1649-54

9 Pencek, R. R., Shearer, J., Camacho, R. C., James, F. D., Lacy, D. B., Fueger, P. T., Donahue, E. P., Snead, W. and Wasserman, D. H. (2005) 5-Aminoimidazole-4-carboxamide-1-beta-D-ribofuranoside causes acute hepatic insulin resistance in vivo. Diabetes 54, 355-60

10 Hardie, D. G., Hawley, S. A. and Scott, J. W. (2006) AMP-activated protein kinase - development of the energy sensor concept. J. Physiol. 574, 7-15

11 Viollet, B., Foretz, M., Guigas, B., Horman, S., Dentin, R., Bertrand, L., Hue, L. and Andreelli, F. (2006) Activation of AMP-activated protein kinase in the liver: a new strategy for the management of metabolic hepatic disorders. J. Physiol. 574, 41-53

12 Reznick, R. M. and Shulman, G. I. (2006) The role of AMP-activated protein kinase in mitochondrial biogenesis. J. Physiol. 574, 33-9

13 Bergeron, R., Ren, J. M., Cadman, K. S., Moore, I. K., Perret, P., Pypaert, M., Young, L. H., Semenkovich, C. F. and Shulman, G. I. (2001) Chronic activation of AMP kinase results in NRF-1 activation and mitochondrial biogenesis. Am. J. Physiol. Endocrinol. Metab. 281, E1340-6

14 Zong, H., Ren, J. M., Young, L. H., Pypaert, M., Mu, J., Birnbaum, M. J. and Shulman, G. I. (2002) AMP kinase is required for mitochondrial biogenesis in skeletal muscle in response to chronic energy deprivation. Proc. Natl. Acad. Sci. U S A 99, 15983-7

15 Guigas, B., Bertrand, L., Taleux, N., Foretz, M., Wiernsperger, N., Vertommen, D., Andreelli, F., Viollet, B. and Hue, L. (2006) 5-Aminoimidazole-4-carboxamide-1-beta-D-ribofuranoside and metformin inhibit hepatic glucose phosphorylation by an AMP-activated protein kinase-independent effect on glucokinase translocation. Diabetes 55, 865-74

16 Viollet, B., Andreelli, F., Jorgensen, S. B., Perrin, C., Geloen, A., Flamez, D., Mu, J., Lenzner, C., Baud, O., Bennoun, M., Gomas, E., Nicolas, G., Wojtaszewski, J. F., Kahn, A., Carling, D., Schuit, F. C., Birnbaum, M. J., Richter, E. A., Burcelin, R. and Vaulont, S. (2003) The AMP-activated protein kinase alpha2 catalytic subunit controls whole-body insulin sensitivity. J. Clin. Invest. 111, 91-8

17 Kellendonk, C., Opherk, C., Anlag, K., Schutz, G. and Tronche, F. (2000) Hepatocyte-specific expression of Cre recombinase. Genesis 26, 151-3
18 Jorgensen, S. B., Viollet, B., Andreelli, F., Frosig, C., Birk, J. B., Schjerling, P., Vaulont, S., Richter, E. A. and Wojtaszewski, J. F. (2004) Knockout of the alpha2 but not alpha1 5'-AMP-activated protein kinase isoform abolishes 5-aminoimidazole-4-carboxamide-1-beta-4-ribofuranoside but not contraction-induced glucose uptake in skeletal muscle. J. Biol. Chem. 279, 1070-9
19 Bontemps, F., Hue, L. and Hers, H. G. (1978) Phosphorylation of glucose in isolated rat hepatocytes. Sigmoidal kinetics explained by the activity of glucokinase alone. Biochem. J. 174, 603-11
20 Klingenberg, M. and Slenczka, W. (1959) [Pyridine nucleotide in liver mitochondria. An analysis of their redox relationships.]. Biochem. Z. 331, 486-517
21 Guigas, B., Detaille, D., Chauvin, C., Batandier, C., De Oliveira, F., Fontaine, E. and Leverve, X. (2004) Metformin inhibits mitochondrial permeability transition and cell death: a pharmacological in vitro study. Biochem. J. 382, 877-84
22 Srere, P. A. (1969) Methods in Enzymology, vol. 13, Academic Press, New York
23 Ichai, C., Guignot, L., El-Mir, M. Y., Nogueira, V., Guigas, B., Chauvin, C., Fontaine, E., Mithieux, G. and Leverve, X. M. (2001) Glucose 6-phosphate hydrolysis is activated by glucagon in a low temperature-sensitive manner. J. Biol. Chem. 276, 28126-33
24 Itaya, K. and Ui, M. (1966) A new micromethod for the colorimetric determination of inorganic phosphate. Clin. Chim. Acta 14, 361-6
25 Van den Berghe, G., Bronfman, M., Vanneste, R. and Hers, H. G. (1977) The mechanism of adenosine triphosphate depletion in the liver after a load of fructose. A kinetic study of liver adenylate deaminase. Biochem. J. 162, 601-9
26 Maswoswe, S. M., Daneshmand, F. and Davies, D. R. (1986) Metabolic effects of D-glyceraldehyde in isolated hepatocytes. Biochem. J. 240, 771-6
27 Vincent, M. F., Erion, M. D., Gruber, H. E. and Van den Berghe, G. (1996) Hypoglycaemic effect of AICAriboside in mice. Diabetologia 39, 1148-55
28 Smith, C. M., Rovamo, L. M. and Raivio, K. O. (1977) Fructose-induced adenine nucleotide catabolism in isolated rat hepatocytes. Can. J. Biochem. 55, 1237-40
29 Van den Berghe, G., Bontemps, F. and Hers, H. G. (1980) Purine catabolism in isolated rat hepatocytes. Influence of coformycin. Biochem. J. 188, 913-20
30 Brown, G. C., Lakin-Thomas, P. L. and Brand, M. D. (1990) Control of respiration and oxidative phosphorylation in isolated rat liver cells. Eur. J. Biochem. 192, 355-62
31 Leverve, X. M. and Fontaine, E. (2001) Role of substrates in the regulation of mitochondrial function in situ. IUBMB Life 52, 221-9
32 Meisse, D., Van de Casteele, M., Beauloye, C., Hainault, I., Kefas, B. A., Rider, M. H., Foufelle, F. and Hue, L. (2002) Sustained activation of AMP-activated protein kinase induces c-Jun N-terminal kinase activation and apoptosis in liver cells. FEBS Lett. 526, 38-42
33 Kefas, B. A., Heimberg, H., Vaulont, S., Meisse, D., Hue, L., Pipeleers, D. and Van de Casteele, M. (2003) AICA-riboside induces apoptosis of pancreatic beta cells through stimulation of AMP-activated protein kinase. Diabetologia 46, 250-4
34 Campas, C., Lopez, J. M., Santidrian, A. F., Barragan, M., Bellosillo, B., Colomer, D. and Gil, J. (2003) Acadesine activates AMPK and induces apoptosis in B-cell chronic lymphocytic leukemia cells but not in T lymphocytes. Blood 101, 3674-80
35 Stefanelli, C., Stanic, I., Bonavita, F., Flamigni, F., Pignatti, C., Guarnieri, C. and Caldarera, C. M. (1998) Inhibition of glucocorticoid-induced apoptosis with 5-aminoimidazole-4-carboxamide ribonucleoside, a cell-permeable activator of AMP-activated protein kinase. Biochem. Biophys. Res. Commun. 243, 821-6
36 Stet, E. H., De Abreu, R. A., Bokkerink, J. P., Vogels-Mentink, T. M., Lambooy, L. H., Trijbels, F. J. and Trueworthy, R. C. (1993) Reversal of 6-mercaptopurine and 6-methylmercaptopurine

ribonucleoside cytotoxicity by amidoimidazole carboxamide ribonucleoside in Molt F4 human malignant T-lymphoblasts. Biochem. Pharmacol. 46, 547-50

37 Ido, Y., Carling, D. and Ruderman, N. (2002) Hyperglycemia-induced apoptosis in human umbilical vein endothelial cells: inhibition by the AMP-activated protein kinase activation. Diabetes 51, 159-67

38 Detaille, D., Guigas, B., Chauvin, C., Batandier, C., Fontaine, E., Wiernsperger, N. and Leverve, X. (2005) Metformin prevents high-glucose-induced endothelial cell death through a mitochondrial permeability transition-dependent process. Diabetes 54, 2179-87

39 Vincent, M. F., Bontemps, F. and Van den Berghe, G. (1992) Inhibition of glycolysis by 5-amino-4-imidazolecarboxamide riboside in isolated rat hepatocytes. Biochem. J. 281 (Pt 1), 267-72

40 Longnus, S. L., Wambolt, R. B., Parsons, H. L., Brownsey, R. W. and Allard, M. F. (2003) 5-Aminoimidazole-4-carboxamide 1-beta -D-ribofuranoside (AICAR) stimulates myocardial glycogenolysis by allosteric mechanisms. Am. J. Physiol. Regul. Integr. Comp. Physiol. 284, R936-44

41 Shang, J. and Lehrman, M. A. (2004) Activation of glycogen phosphorylase with 5-aminoimidazole-4-carboxamide riboside (AICAR). Assessment of glycogen as a precursor of mannosyl residues in glycoconjugates. J. Biol. Chem. 279, 12076-80

42 Jacobs, R. L., Lingrell, S., Dyck, J. R. and Vance, D. E. (2006) Inhibition of hepatic phosphatidylcholine synthesis by 5-aminoimidazole-4-carboxamide-1-beta-4-ribofuranoside (AICAr) is independent of AMP-activated protein kinase (AMPK) activation. J. Biol. Chem. Dec 19, M605702200

43 Meley, D., Bauvy, C., Houben-Weerts, J. H., Dubbelhuis, P. F., Helmond, M. T., Codogno, P. and Meijer, A. J. (2006) AMP-activated protein kinase and the regulation of autophagic proteolysis. J. Biol. Chem. 281, 34870-9

44 Wu, Z., Puigserver, P., Andersson, U., Zhang, C., Adelmant, G., Mootha, V., Troy, A., Cinti, S., Lowell, B., Scarpulla, R. C. and Spiegelman, B. M. (1999) Mechanisms controlling mitochondrial biogenesis and respiration through the thermogenic coactivator PGC-1. Cell 98, 115-24

45 Li, F., Wang, Y., Zeller, K. I., Potter, J. J., Wonsey, D. R., O'Donnell, K. A., Kim, J. W., Yustein, J. T., Lee, L. A. and Dang, C. V. (2005) Myc stimulates nuclearly encoded mitochondrial genes and mitochondrial biogenesis. Mol. Cell. Biol. 25, 6225-34

46 Scarpulla, R. C. (2006) Nuclear control of respiratory gene expression in mammalian cells. J. Cell. Biochem. 97, 673-83

47 Woods, A., Azzout-Marniche, D., Foretz, M., Stein, S. C., Lemarchand, P., Ferre, P., Foufelle, F. and Carling, D. (2000) Characterization of the role of AMP-activated protein kinase in the regulation of glucose-activated gene expression using constitutively active and dominant negative forms of the kinase. Mol. Cell. Biol. 20, 6704-11

48 Pilon, G., Dallaire, P. and Marette, A. (2004) Inhibition of inducible nitric-oxide synthase by activators of AMP-activated protein kinase: a new mechanism of action of insulin-sensitizing drugs. J. Biol. Chem. 279, 20767-74

49 Viollet, B., Andreelli, F., Jorgensen, S. B., Perrin, C., Flamez, D., Mu, J., Wojtaszewski, J. F., Schuit, F. C., Birnbaum, M., Richter, E., Burcelin, R. and Vaulont, S. (2003) Physiological role of AMP-activated protein kinase (AMPK): insights from knockout mouse models. Biochem. Soc. Trans. 31, 216-9

50 Cool, B., Zinker, B., Chiou, W., Kifle, L., Cao, N., Perham, M., Dickinson, R., Adler, A., Gagne, G., Iyengar, R., Zhao, G., Marsh, K., Kym, P., Jung, P., Camp, H. S. and Frevert, E. (2006) Identification and characterization of a small molecule AMPK activator that treats key components of type 2 diabetes and the metabolic syndrome. Cell. Metab. 3, 403-16

FIGURES LEGENDS

Figure 1: Time-course of the effects of AICA riboside on intracellular ZMP concentration, AMPK activity and oxygen consumption rate in rat hepatocytes. Hepatocytes isolated from 24h-starved rats were incubated at 37°C in a Krebs/bicarbonate medium supplemented with 20/2 mM lactate/pyruvate and 4 mM octanoate. After 15 min of pre-incubation (time 0), AICA riboside (1 mM final concentration, open squares) or its vehicule (black squares) were added and cell samples were removed at the indicated time for determination of intracellular ZMP content (A), AICA riboside concentration in the medium (B), AMPK activity (C) and phosphorylation state of ACC on Ser79 (C, insert). The oxygen consumption rate (JO_2) was measured in separate experiments before and after the addition of 0.15 μg/ml antimycin. The antimycin-sensitive JO_2 was calculated by subtracting the antimycin-insensitive JO_2. The results are expressed as means ± S.E.M. (n=3-4). *, $p<0.05$ compared with no addition.

Figure 2: Effects of AICA riboside on AMPK activity, intracellular ATP concentration, oligomycin-sensitive oxygen consumption rate in hepatocytes from wild-type and AMPK$\alpha1\alpha2_{LS}^{-/-}$ mice, and determination of hepatic expression of various mitochondrial proteins in both strains. Hepatocytes from wild-type or AMPK$\alpha1\alpha2_{LS}^{-/-}$ mice were incubated with 1 mM AICA riboside (open squares) or the vehicule (black squares), as described in Table 1a. After 30 min, cell samples were removed for AMPK activity (A) and intracellular ATP concentrations (B). The oligomycin-sensitive oxygen consumption rate (JO_2) was measured in separate experiments in wild-type (C) and AMPK$\alpha1\alpha2_{LS}^{-/-}$ mice (D), after the successive addition of 6 μg/ml oligomycin, 100 μM DNP, 0.15 μg/ml antimycin and 1 mM TMPD plus 5 mM ascorbate. The antimycin-sensitive JO_2 was calculated by subtracting the antimycin-insensitive JO_2. The cytochrome c (Cyt. C) and cytochrome oxidase (COX IV) contents in hepatocytes from wild-type (black bars) and AMPK$\alpha_1\alpha_{2LS}^{-/-}$ (hatched bars) mice were evaluated by western blot and quantification was performed by densitometry using actin as loading control (E, F). RNA was extracted from freeze-clamped livers of wild-type (black bars) and AMPK$\alpha_1\alpha_{2LS}^{-/-}$ (hatched bars) mice starved for 24h. Quantitative real-time PCR was performed on cDNA and the mRNA contents for the indicated gene (G) were normalized for β-actin and expressed relative to that in wild-type mice. The results of all experiments are expressed as

means ± S.E.M. (n=3-5). *, $p<0.05$ compared with no addition. $, $p<0.05$ compared with wild-type mice.

Figure 3: Relationship between intracellular Pi and the oligomycin-sensitive respiration in hepatocytes. Hepatocytes were incubated as described in Table 5 with (open symbols) or without 1 mM AICA riboside (closed symbols) and in presence of fructose (squares), deoxycoformycin (triangles) or vehicule (circles). The results are expressed as means ± S.E.M. (n=3).

Table 1a

Dose-dependent effects of AICA riboside on AMPK activity, ZMP concentration and oxygen consumption rate in isolated rat hepatocytes. Hepatocytes isolated from 24h-starved rats were incubated at 37°C in a Krebs/bicarbonate medium supplemented with 20/2 mM lactate/pyruvate and 4 mM octanoate and in presence or not of the indicated concentrations of AICA riboside. After 30 min of incubation, the antimycin-sensitive oxygen consumption rate (JO_2) was measured before and after the successive addition of 6 μg/ml oligomycin, 100 μM DNP, 0.15 μg/ml antimycin and 1 mM TMPD plus 5 mM ascorbate. The oligomycin-sensitive JO_2 was calculated by subtracting the oligomycin-insensitive from the basal JO_2. In separate experiments, samples of cell suspension were removed for AMPK assay and determination of intracellular ZMP concentrations, as described in the Materials and Methods section. The results are expressed as means ± S.E.M. (n=4). *, $p<0.05$ compared with no addition.

AICA riboside (μM)	ZMP (μmol.g dry hepatocytes^{-1})	AMPK activity (U.g dry hepatocytes^{-1})	JO_2 (μmol O_2.min^{-1}.g dry hepatocytes^{-1})				
			Basal	Oligomycin	Oligomycin-sensitive	DNP	TMPD/a
0	< 0.1	123 ± 6	26.4 ± 1.3	9.9 ± 0.8	16.5 ± 1.0	44.3 ± 3.8	108.2 ± 7.1
50	1.2 ± 0.1*	145 ± 7*	22.4 ± 1.7*	10.0 ± 0.3	12.3 ± 1.4*	40.7 ± 1.3	108.0 ± 2.0
100	2.1 ± 0.1*	175 ± 7*	23.1 ± 1.2*	9.0 ± 0.8	14.1 ± 0.9*	41.2 ± 4.8	105.9 ± 6.2
250	6.1 ± 0.7*	217 ± 8*	20.9 ± 0.9*	9.9 ± 1.2	11.0 ± 0.5*	42.0 ± 5.9	99.6 ± 8.7
500	10.5 ± 1.3*	245 ± 8*	18.5 ± 0.9*	8.8 ± 0.7	9.7 ± 0.8*	38.8 ± 5.3	99.9 ± 8.8
1000	15.0 ± 1.4*	220 ± 12*	18.1 ± 0.4*	8.5 ± 1.1	9.6 ± 1.0*	38.6 ± 5.7	101.9 ± 6.7
2500	17.0 ± 1.0*	211 ± 9*	16.5 ± 1.0*	7.5 ± 0.9*	9.0 ± 0.6*	35.2 ± 5.7*	97.7 ± 6.0

Table 1b

Dose-dependent effects of AICA riboside on adenine nucleotide and inorganic phosphate concentrations in isolated rat hepatocytes. Hepatocytes isolated from 24h-starved rats were incubated as described in Table 1a. After 30 min of incubation, samples of cell suspension were removed for determination of intracellular adenine nucleotide and inorganic phosphate concentrations, as described in the Materials and Methods section. The results are expressed as means ± S.E.M. (n=3-4). *, $p<0.05$ compared with no addition; nd : not determined.

AICA riboside (μM)	ATP	ADP	AMP	ΣAN	Pi	ATP/ADP
	(μmol.g dry hepatocytes^{-1})					
0	9.5 ± 0.3	0.7 ± 0.0	2.9 ± 0.5	13.2 ± 0.8	11.8 ± 0.6	14.4 ± 0.9
50	8.7 ± 0.5	0.8 ± 0.1	2.3 ± 0.3	11.7 ± 0.7	nd	13.2 ± 2.0
100	8.8 ± 0.6	0.7 ± 0.1	2.6 ± 0.5	12.2 ± 1.1	11.5 ± 0.9	13.4 ± 1.7
250	8.1 ± 0.6*	0.8 ± 0.1*	2.0 ± 0.2*	11.3 ± 0.7*	nd	10.4 ± 1.0*
500	8.0 ± 0.6*	0.9 ± 0.1*	1.6 ± 0.3*	10.4 ± 0.9*	4.2 ± 0.5*	9.5 ± 1.1*
1000	7.4 ± 0.7*	1.2 ± 0.2*	1.7 ± 0.3*	9.9 ± 1.0*	3.7 ± 0.6*	8.0 ± 1.3*
2500	7.2 ± 0.8*	1.1 ± 0.2*	1.6 ± 0.3*	9.9 ± 1.3*	3.4 ± 0.2*	7.4 ± 1.4*

Table 2: Effects of AICA riboside on oligomycin-sensitive and uncoupled oxygen consumption rate in isolated rat hepatocytes incubated with different substrates. Hepatocytes isolated from 24h-starved rats were incubated at 37°C in a Krebs/bicarbonate medium in presence or not of 1 mM AICA riboside. Experiments were performed either without the addition of exogenous substrate or in the presence of 20 mM glycerol, 20 mM glucose, 20/2 mM lactate/pyruvate and 4 mM octanoate as indicated. After 30 min, the oligomycin-sensitive and uncoupled oxygen consumption rate (JO_2) was determined after addition of 6 μg/ml oligomycin and 100 μM DNP, respectively. The results are expressed as means ± S.E.M. (n=4). *, $p<0.05$ compared with no addition.

		JO_2 (μmol.min^{-1}.g dry hepatocytes^{-1})	
	AICA riboside	**Oligomycin-sensitive**	**DNP**
Endogenous	-	3.1 ± 0.3	16.7 ± 1.0
	+	2.4 ± 0.4 *	17.0 ± 0.7
Glycerol	-	5.4 ± 0.5	19.9 ± 0.7
	+	4.3 ± 0.4 *	21.8 ± 1.0
Glucose	-	6.8 ± 0.8	26.1 ± 0.5
	+	2.9 ± 0.2 *	19.3 ± 1.5 *
Glucose + Octanoate	-	12.8 ± 1.2	32.6 ± 3.5
	+	7.9 ± 0.5 *	28.0 ± 0.8
Lactate + Pyruvate + Octanoate	-	15.2 ± 1.0	43.5 ± 3.7
	+	6.3 ± 0.7 *	40.7 ± 7.1

Table 3

Effects of AICA riboside on mitochondrial oxidative phosphorylation in permeabilized hepatocytes from wild-type and AMPK$\alpha_1\alpha_{2LS}^{-/-}$ mice. Hepatocytes from wild-type (WT) and AMPK$\alpha_1\alpha_{2LS}^{-/-}$ mice were incubated at 37°C in presence or not of 1 mM AICA riboside, as described in the Table 1a, and then permeabilized in a KCl medium containing 200 μg/ml digitonin. After 3 min, cells were transferred in an oxygraph vessel and "*in situ*" mitochondria were energized with either 5 mM glutamate + 2.5 mM malate or 5 mM succinate + 0.5 mM malate + l.25 μM rotenone. The state 3 respiratory rate was obtained by the addition of 1 mM ADP, the state 4 respiratory rate by the addition of 6 μg/ml oligomycin and the uncoupled respiratory rate by the addition of 75 μM DNP. The maximal activity of cytochrome oxidase was obtained by the addition of 1 mM TMPD and 5 mM ascorbate, in the presence of 0.15 μg/ml antimycin. The antimycin-sensitive respiratory rate was calculated by subtracting the antimycin-insensitive respiratory rate. The results are expressed as means ± S.E.M. (n=4-5 in each group). $, $p<0.05$ compared with Wild-Type; nd : not determined.

	AICA riboside	Respiratory rate (natoms O.min^{-1}.mg proteins^{-1})			
		State 3	State 4	DNP	TMPD/a
Glutamate/malate					
Wild-type	-	62.6 ± 9.0	7.7 ± 1.4	50.5 ± 8.1	147.3 ± 23.0
	+	52.3 ± 8.6	6.3 ± 0.5	44.1 ± 9.5	140.5 ± 18.5
AMPK$\alpha_1\alpha_{2LS}^{-/-}$	-	27.7 ± 8.9$^{\$}$	3.1 ± 0.5$^{\$}$	25.1 ± 8.4$^{\$}$	89 ± 17.3$^{\$}$
	+	16.2 ± 8.4$^{\$}$	2.1 ± 0.5$^{\$}$	14.7 ± 7.9$^{\$}$	67.5 ± 19.4$^{\$}$
Succinate/malate					
Wild-type	-	68.5 ± 9.9	20.7 ± 2.3	55.4 ± 9.0	nd
	+	71.6 ± 12.6	22.5 ± 3.2	58.1 ± 11.7	nd
AMPK$\alpha_1\alpha_{2LS}^{-/-}$	-	29.3 ± 8.9$^{\$}$	10.5 ± 2.6$^{\$}$	27.2 ± 8.4$^{\$}$	nd
	+	22.0 ± 8.4$^{\$}$	8.4 ± 2.6$^{\$}$	19.4 ± 8.4$^{\$}$	nd

Table 4

Effects of AICA riboside and Z nucleotides on oxidative phosphorylation in rat isolated mitochondria. Isolated rat mitochondria (1 mg/ml) were incubated at 37°C in a KCl medium in presence of 1 mM AICA riboside, the indicated concentrations of nucleotides or the vehicule. Mitochondria were energized with either 5 mM glutamate + 2.5 mM malate or 5 mM succinate + 0.5 mM malate + l.25 μM rotenone. The state 3 respiratory rate was obtained by the addition of 1 mM ADP, the state 4 respiratory rate by the addition of 6 μg/ml oligomycin and the uncoupled respiratory rate by the addition of 75 μM DNP. Antimycin-sensitive oxygen consumption rate was calculated by subtracting the antimycin-insensitive respiratory rate after addition of 0.15 μg/ml antimycin. The results are expressed as means ± S.E.M. (n=3-4 different preparations, each assay being performed in duplicate). *, $p<0.05$ compared with control-vehicule.

	Respiratory rate (natoms $O.min^{-1}.mg\ proteins^{-1}$)		
	State 3	**State 4**	**DNP**
Glutamate/malate			
Control	80.7 ± 3.0	15.9 ± 0.6	126.0 ± 5.9
AICA riboside	80.5 ± 8.2	16.4 ± 0.9	120.0 ± 14.2
1 mM ZMP	74.0 ± 1.3*	15.4 ± 0.3	105.3 ± 1.2*
2.5 mM ZMP	61.5 ± 5.0*	15.7 ± 1.5	98.6 ± 4.2*
0.5 mM ZTP	97.1 ± 8.7*	19.7 ± 0.8*	138.5 ± 9.2*
1 mM ZTP	105.1 ± 8.4*	23.7 ± 1.6*	144.3 ± 13.0*
Succinate/malate			
Control	122.9 ± 0.6	37.6 ± 0.2	158.0 ± 7.1
AICA riboside	120.0 ± 3.0	35.6 ± 0.9	143.1 ± 4.9
1 mM ZMP	122.3 ± 4.7	34.8 ± 0.7	140.7 ± 1.2
0.5 mM ZTP	122.1 ± 5.5	41.9 ± 2.1*	210.2 ± 9.5*

Table 5

Effects of fructose and deoxycoformycin on the AICA riboside-induced decrease in oligomycin-sensitive oxygen consumption rate and adenine nucleotide, ZMP and inorganic phosphate concentrations in rat hepatocytes. Hepatocytes isolated from 24h-starved rats were incubated at 37°C in a Krebs/bicarbonate medium supplemented with 20/2 mM lactate/pyruvate and 4 mM octanoate in presence or not of 5 mM fructose or 10 μM deoxycoformycin. After 15 min of pre-incubation, AICA riboside (1 mM final concentration) or its vehicule were added and cell samples were removed 30 min later for determination of the oligomycin-sensitive oxygen consumption rate (JO_2, A), as described in the Legend of Figure 2. Determination of adenine nucleotides, ZMP and Pi were performed in separate experiments. The results are expressed as means ± S.E.M. (n=3). *, $p<0.05$ compared with no AICA riboside addition; $, $p<0.05$ compared with control incubated in the same condition.

	AICA riboside	ZMP (μmol.g dry hepatocytes^{-1})	JO_2 (μmol.min^{-1}.g dry hepatocytes^{-1})	ATP	ADP	AMP	ΣAN	Pi	ATP/ADP
				(μmol.g dry hepatocytes^{-1})					
Control	-	< 0.1	17.8 ± 0.4	10.4 ± 0.4	0.9 ± 0.1	3.5 ± 0.3	15.1 ± 0.5	12.6 ± 0.1	13.2 ± 1.6
	+	21.2 ± 1.1*	8.7 ± 0.6*	8.4 ± 0.5*	1.7 ± 0.1*	2.5 ± 0.2*	12.2 ± 0.7*	4.4 ± 0.1*	5.1 ± 0.4*
Fructose	-	< 0.1	20.0 ± 1.1$^{\$}$	7.4 ± 0.4$^{\$}$	1.0 ± 0.1	2.8 ± 0.2$^{\$}$	11.3 ± 0.6$^{\$}$	17.4 ± 0.8$^{\$}$	8.7 ± 1.3$^{\$}$
	+	6.1 ± 0.1*$^{\$}$	7.4 ± 0.6*$^{\$}$	3.3 ± 0.2*$^{\$}$	1.7 ± 0.2*	2.9 ± 0.2	7.7 ± 0.5*$^{\$}$	2.4 ± 0.3*$^{\$}$	2.1 ± 0.2*$^{\$}$
Deoxycoformycin	-	< 0.1	15.0 ± 0.3$^{\$}$	12.3 ± 0.2$^{\$}$	1.2 ± 0.1$^{\$}$	4.3 ± 0.2$^{\$}$	18.2 ± 0.3$^{\$}$	11.3 ± 0.3$^{\$}$	12.1 ± 1.0
	+	13.2 ± 0.3*$^{\$}$	8.5 ± 0.8*	12.9 ± 0.2$^{\$}$	3.0 ± 0.1*$^{\$}$	3.7 ± 0.4$^{\$}$	19.5 ± 0.5$^{\$}$	4.3 ± 0.3*	4.7 ± 0.2*

Biochemical Journal Immediate Publication. Published on 27 Feb 2007 as manuscript BJ20070105

Figure 1

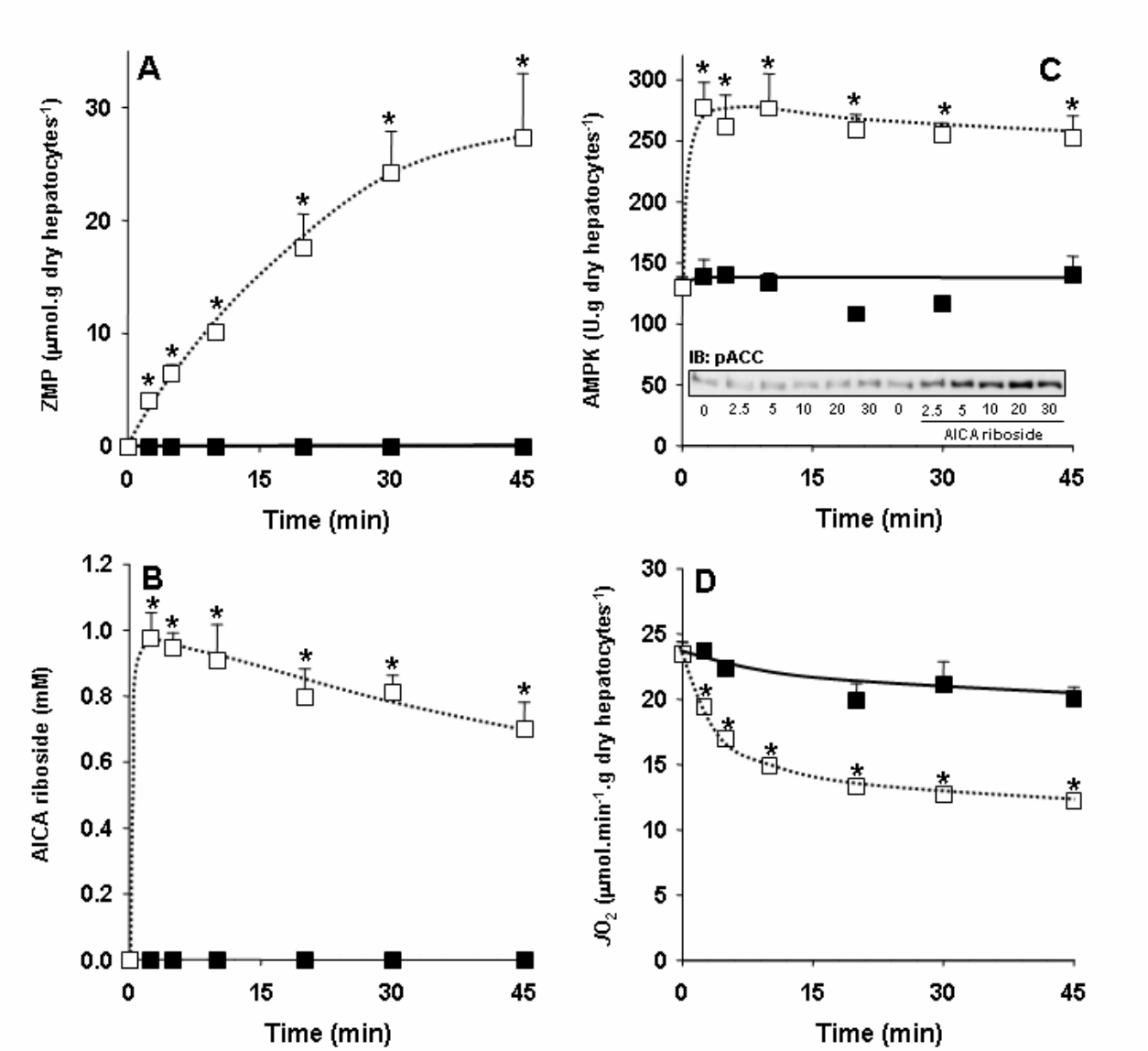

Figure 2

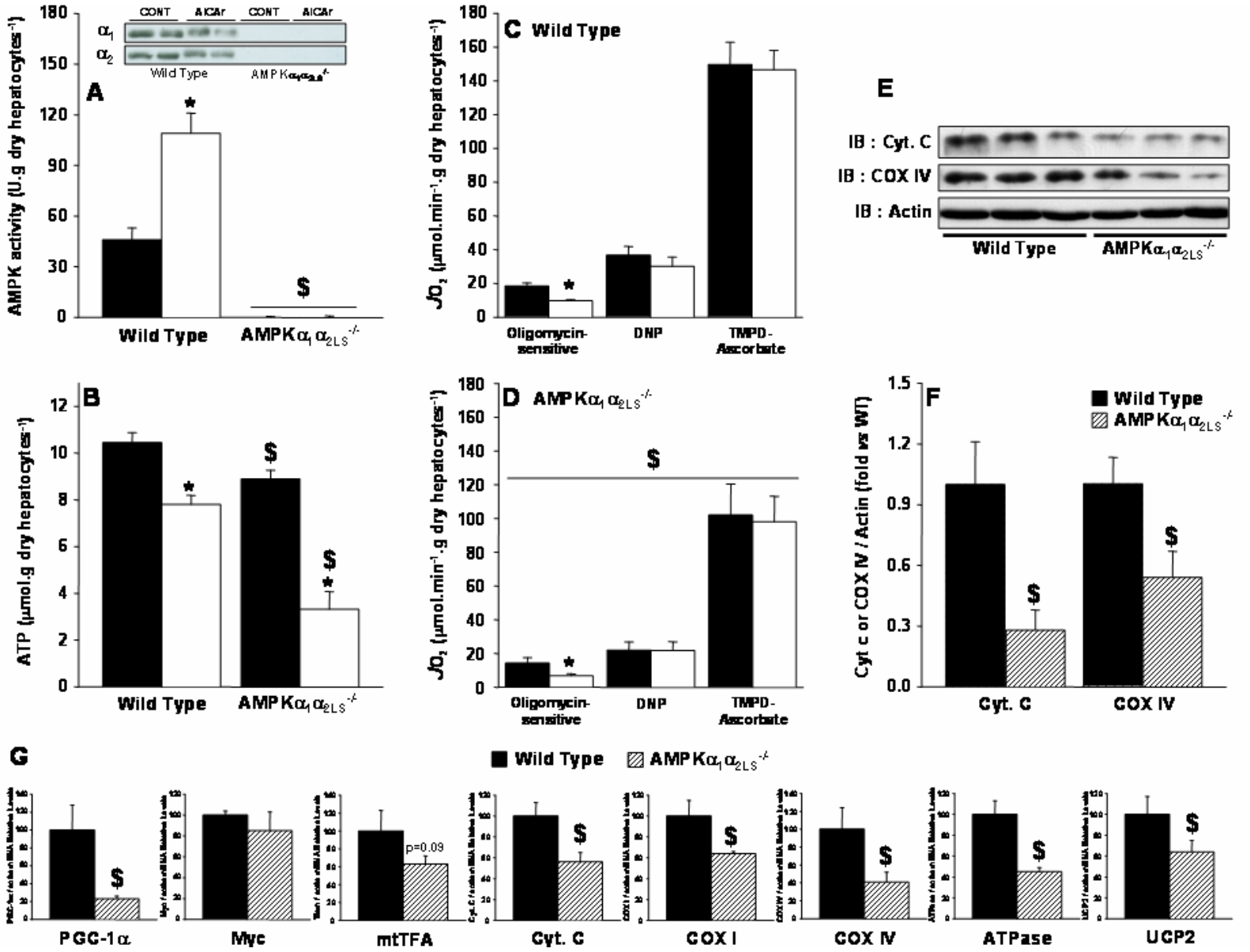

Figure 3